

A Novel Intrinsic Measure of Data Separability

Shuyue Guan · Murray Loew

Received: date / Accepted: date

Abstract In machine learning, the performance of a classifier depends on both the classifier model and the separability/complexity of datasets. To quantitatively measure the separability of datasets, we create an *intrinsic measure* – the Distance-based Separability Index (DSI), which is independent of the classifier model. We consider the situation in which different classes of data are mixed in the same distribution to be the most difficult for classifiers to separate. We then formally show that the DSI can indicate whether the distributions of datasets are identical for any dimensionality. And we verify the DSI to be an effective separability measure by comparing to several state-of-the-art separability/complexity measures using synthetic and real datasets. Having demonstrated the DSI’s ability to compare distributions of samples, we also discuss some of its other promising applications, such as measuring the performance of generative adversarial networks (GANs) and evaluating the results of clustering methods.

Keywords data complexity · data separability measure · learning difficulty · machine learning

Declarations Not applicable.

Shuyue Guan
ORCID: [0000-0002-3779-9368](https://orcid.org/0000-0002-3779-9368)
E-mail: frankshuyueguan@gwu.edu

Murray Loew
Corresponding author
E-mail: loew@gwu.edu

Department of Biomedical Engineering,
George Washington University, Washington DC, USA

1 Introduction

Data and models are the two main foundations of machine learning and deep learning. Models learn knowledge (patterns) from datasets. An example is that the convolutional neural network (CNN) classifier learns how to recognize images from different classes. There are two aspects in which we examine the learning process: capability of the classifier and the separability of dataset. Separability is an intrinsic characteristic of a dataset [6] to describe how data points belonging to different classes mix with each other. The learning outcomes are highly dependent on the two aspects. For a specific model, the learning capability is fixed, so that the training process depends on the training data. As reported by Chiyuan et al. [30], the time to convergence for the same training loss on random labels on the CIFAR-10 dataset was greater than when training on true labels. It is not surprising that the performance of a given model varies between different training datasets depending on their separability. For example, in a two-class problem, if the scattering area for each class has no overlap, one straight line (or hyperplane) can completely separate the data points (Figure 1a). For the distribution shown in Figure 1b, however, a single straight line cannot separate the data points successfully, but a combination of many lines can.



Fig. 1: Different separability of two datasets

In machine learning, for a given classifier, it is more difficult to train on some datasets than on others. The difficulty of training on a less-separable dataset is made evident by the requirement for greater learning times (*e.g.*, number of epochs for deep learning) to reach the same accuracy (or loss) value and/or to obtain a lower accuracy (or higher loss), compared with the more-separable dataset. The training difficulty, however, also depends on the model employed. Hence, an intrinsic measure of separability that is independent of the model is required. In other words, it is very useful to be able to measure the separability of a dataset without using a classifier model. In summary, the separability of a dataset can be characterized in three ways:

1. To describe how data points belonging to different classes mix with each other.
2. To determine the number of [hyper-] planes/linear-dividers needed to separate different-class data points.
3. To gain insights into the training of a specific classifier with regard to time-cost and final accuracy.

Our proposed method is based on the first way. The second and third ways depend on classifiers; we used the third way to verify our method.

1.1 Related work

A review of the literature indicates that there have been substantially fewer studies on data separability *per se* than on classifiers. The Fisher discriminant ratio (FDR) [16] measures the separability of data using the mean and standard deviation (SD) of each class. It has been used in many studies, but it fails in some cases (*e.g.*, as Figure 5(e) shows, Class 1 data points are scattered around Class 2 data points in a circle; their $FDR \approx 0$). A more general issue than that of data separability is data complexity, which measures not only the relationship between classes but also the data distribution in feature space. Ho and Basu [14] conducted a groundbreaking review of data complexity measures. They reported measures for classification difficulty, including those associated with the geometrical complexity of class boundaries. Recently, Lorena et al. [17] summarized existing methods for the measurement of classification complexity. In the survey, most complexity measures have been grouped in six categories: *feature-based*, *linearity*, *neighborhood*, *network*, *dimensionality*, and *class imbalance* measures (Table 1). For example, the FDR is a *feature-based* measure, and the geometric separability index (GSI) proposed by Thornton [28] is considered a *neighborhood* measure. Other ungrouped

measures discussed in Lorena’s paper have similar characteristics to the grouped measures or may have large time cost. Each of these methods has possible drawbacks. In particular, the features extracted from data for the five categories of *feature-based* measures may not accurately describe some key characteristics of the data; some *linearity* measures depend on the classifier used, such as support-vector machines (SVMs); *neighborhood* measures may show only local information; some *network* measures may also be affected by local relationships between classes depending on the computational methods employed; *dimensionality* measures are not strongly related to classification complexity; and, *class imbalance* measures do not take the distribution of data into account.

Table 1: Complexity measures reported by Lorena et al. [17]

Category	Name	Code
Feature-based	Maximum Fisher’s discriminant ratio	F1
	Directional vector maximum Fisher’s discriminant ratio	F1v
	Volume of overlapping region	F2
	Maximum individual feature efficiency	F3
	Collective feature efficiency	F4
Linearity	Sum of the error distance for linear programming	L1
	Error rate of the linear classifier	L2
	Non-linearity of the linear classifier	L3
Neighborhood	Fraction of borderline points	N1
	Ratio of intra/extra class NN distance	N2
	Error rate of the NN classifier	N3
	Non-linearity of the NN classifier	N4
	Fraction of hyperspheres covering the data	T1
	Local set average cardinality	LSC
Network	Density	Density
	Clustering coefficient	ClsCoef
	Hubs	Hubs
Dimensionality	Average number of features per dimension	T2
	Average number of PCA dimensions per point	T3
	Ratio of the PCA dimension to the original dimension	T4
Class imbalance	Entropy of class proportions	C1
	Imbalance ratio	C2

In this paper, we create a novel separability measure for multi-class datasets and verify it by comparing with other separability/complexity measures using synthetic and real (CIFAR-10/100) datasets. Since several previous studies [28, 19, 1, 23, 18] have used the term separability index (SI), we refer to our measure as the distance-based separability index (DSI). The DSI measure is similar in some respects to the *network* measures because it represents the universal relations be-

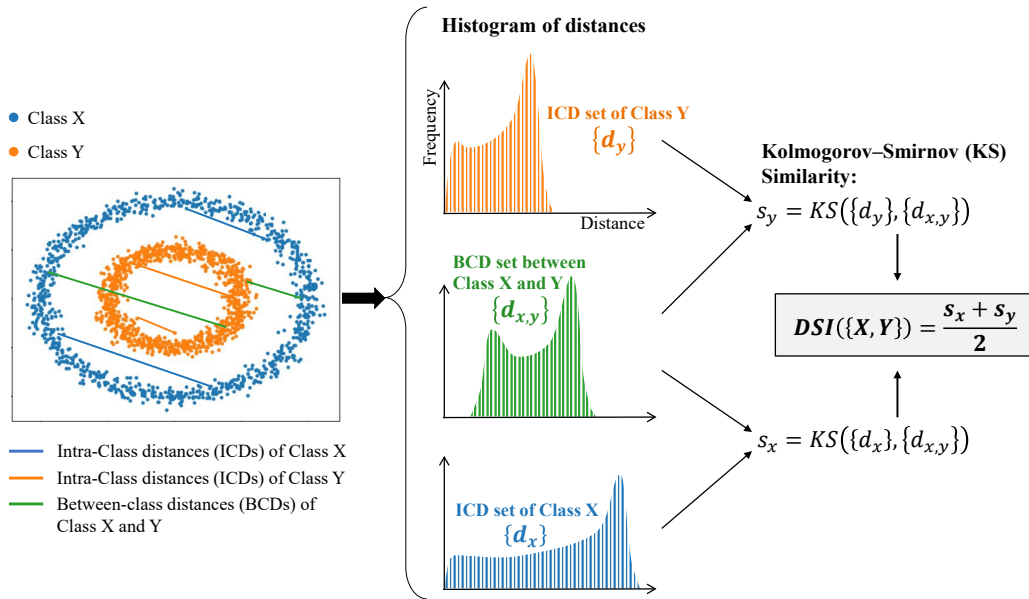


Fig. 2: An example of two-class dataset in 2-D shows the definition and computation of the DSI. Details about the ICD and BCD sets are in Section 2.1, and Section 2.2 contains more details about computation of the DSI. The proof that DSI can measure the separability of dataset is shown in Section 2.3.

tween the data points. Especially, we have formally shown that the DSI can indicate whether the distributions of datasets are identical for any dimensionality. Figure 2 shows the definition and computation of the DSI by an example of a two-class dataset in 2-D. In general, the DSI has a wide applicability and is not limited to simply understanding the data; for example, it can also be applied to measure generative adversarial network (GAN) performance [12], evaluate clustering results [11], anomaly detection [22], the selection of classifiers [20, 3, 4, 8], and features for classification [27, 5].

The novelty of this study is the examination of the 1) distributions of datasets via 2) the distributions of distances between data points in datasets; the proved Theorem connects the two kinds of distributions; that is the gist of DSI. To the best of our knowledge, none of the existing studies uses the same methods.

2 Methodological Development for DSI

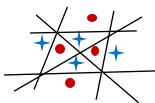


Fig. 3: Two-class dataset with maximum entropy

In a two-class dataset, we consider that the most difficult situation to separate the data is when the two classes of data are scattered and mixed together with the same distribution. In this situation, the proportion of each class in every small region is equal, and the system has maximum entropy. In extreme cases, to obtain 100% classification accuracy, the classifier must separate each data point into an individual region (Figure 3).

Therefore, one possible definition of data separability is the inverse of a system's entropy. To calculate entropy, the space could be randomly divided into many small regions. Then, the proportions of each class in every small region can be considered as their occurrence probabilities. The system's entropy can be derived from those probabilities [26]. In high-dimensional space (*e.g.*, image data), however, the number of small regions grows exponentially. For example, the space for 32×32 pixels 8-bit RGB images has 3,072 dimensions. If each dimension (ranging from 0 to 255, integer) is divided into 32 intervals, the total number of small regions is $32^{3072} \approx 6.62 \times 10^{4623}$. It is thus impossible to compute the system's entropy and analyze data separability in this way.

Alternatively, we can define the data separability as the similarity of data distributions. If a dataset contains two classes X and Y with the same distribution (distributions have the same shape, position and support, *i.e.* the same probability density function) and

have sufficient data points to fill the region, this dataset reaches the maximum entropy because within any small regions, the occurrence probabilities of the two classes data are equal (50%). It is also the most difficult situation for separation of the dataset.

Here, we proposed a new method – distance-based separability index (DSI) to measure the similarity of data distributions. DSI is used to analyze how two classes of data are mixed together, as a substitute for entropy.

2.1 Intra-class and between-class distance sets

Before introducing the DSI, we introduce the intra-class distance (ICD) and the between-class distance (BCD) set that are used for computation of the DSI. The “set” in this paper means the *multiset* that allows duplicate elements (distance values, in our cases), and the $|A|$ of a “set” A is the number of its elements.

Suppose X and Y have N_x and N_y data points, respectively, we can define:

Definition 1 The intra-class distance (ICD) set $\{d_x\}$ is a set of distances between any two points in the same class (X), as: $\{d_x\} = \{\|x_i - x_j\|_2 | x_i, x_j \in X; x_i \neq x_j\}$.

Corollary 1 Given $|X| = N_x$, then $|\{d_x\}| = \frac{1}{2}N_x(N_x - 1)$.

Definition 2 The between-class distance (BCD) set $\{d_{x,y}\}$ is the set of distances between any two points from different classes (X and Y), as $\{d_{x,y}\} = \{\|x_i - y_j\|_2 | x_i \in X; y_j \in Y\}$.

Corollary 2 Given $|X| = N_x, |Y| = N_y$, then $|\{d_{x,y}\}| = N_x N_y$.

Remark 1 The metric for all distances is *Euclidean* (l^2 norm) in this paper. In Section 4.1.1, we compare the Euclidean distance with some other distance metrics including City-block, Chebyshev, Correlation, Cosine, and Mahalanobis, and we showed that the DSI based on Euclidean distance has the best sensitivity to complexity, and thus we selected it.

2.2 Definition and computation of the DSI

We firstly introduce the computation of the DSI for a dataset contains only two classes X and Y :

1. First, the ICD sets of X and Y : $\{d_x\}, \{d_y\}$ and the BCD set: $\{d_{x,y}\}$ are computed by their definitions (Defs. 1 and 2).

2. Second, the similarities between the ICD and BCD sets are then computed using the the Kolmogorov–Smirnov (KS) [7] distance¹:

$$s_x = KS(\{d_x\}, \{d_{x,y}\}), \text{ and } s_y = KS(\{d_y\}, \{d_{x,y}\}).$$

We explain the reasons to choose the KS distance in Section 4.1.

3. Finally, the DSI is the average of the two KS distances:

$$DSI(\{X, Y\}) = \frac{(s_x + s_y)}{2}.$$

Remark 2 We do not use the weighted average because once the distributions of the ICD and BCD sets can be well characterized, the sizes of X and Y will not affect the KS distances s_x and s_y .

For a multi-class dataset, the DSI can be computed by one-*versus*-others; specifically, for a n -class dataset, the process to obtain its DSI is:

1. Compute n ICD sets for each class: $\{d_{C_i}\}; i = 1, 2, \dots, n$, and compute n BCD sets for each class. For the i -th class of data C_i , the BCD set is the set of distances between any two points in C_i and $\overline{C_i}$ (other classes, not C_i): $\{d_{C_i, \overline{C_i}}\}$.
2. Compute the n KS distances between ICD and BCD sets for each class:

$$s_i = KS(\{d_{C_i}\}, \{d_{C_i, \overline{C_i}}\}).$$

3. Calculate the average of the n KS distances; the DSI of this dataset is:

$$DSI(\{C_i\}) = \frac{\sum s_i}{n}.$$

Therefore, DSI is (defined as) the mean value of KS distances between the ICD and BCD sets for each class of data in a dataset.

Remark 3 $DSI \in (0, 1)$. A small DSI (low separability) means that the ICD and BCD sets are very similar. In this case, by Theorem 1, the distributions of datasets are similar too. Hence, these datasets are difficult to separate.

¹ In experiments, we used the `scipy.stats.ks_2samp` from the SciPy package in Python to compute the KS distance. https://docs.scipy.org/doc/scipy/reference/generated/scipy.stats.ks_2samp.html

2.3 Theorem: DSI and similarity of data distributions

Then, the Theorem 1 shows how the ICD and BCD sets are related to the distributions of the two-class data; it demonstrates the core value of this study.

Theorem 1 *When $|X|$ and $|Y| \rightarrow \infty$, if and only if the two classes X and Y have the same distribution, the distributions of the ICD and BCD sets are identical.*

The full proof of Theorem 1 is in Section 2.4. Here we provide an informal explanation:

Data points in X and Y having the same distribution can be considered to have been sampled from one distribution Z . Hence, both ICDs of X and Y , and BCDs between X and Y are actually ICDs of Z . Consequently, the distributions of ICDs and BCDs are identical. In other words, that the distributions of the ICD and BCD sets are identical indicates all labels are assigned randomly and thus, the dataset has the least separability.

According to this theorem, that the distributions of the ICD and BCD sets are identical indicates that the dataset has maximum entropy because X and Y have the same distribution. Thus, as we discussed before, the dataset has the lowest separability. And in this situation, the dataset's DSI ≈ 0 by its definition.

The time costs for computing the ICD and BCD sets increase linearly with the number of dimensions and quadratically with the number of data points. It is much better than computing the dataset's entropy by dividing the space into many small regions. Our experiments (in Section 3.2.1) show that the time costs could be greatly reduced using a small random subset of the entire dataset without significantly affecting the results (Figure 8). And in practice, the computation of DSI can be sped-up considerably by using tensor-based matrix multiplications on a GPU (*e.g.*, it takes about 2.4 seconds for 4000 images from CIFAR-10 running on a GTX 1080 Ti graphics card) because the main time-cost is the computation of distances.

2.4 Proof of Theorem 1

Consider two classes X and Y that have the same distribution (distributions have the same shape, position, and support, *i.e.*, the same probability density function) and have sufficient data points ($|X|$ and $|Y| \rightarrow \infty$) to fill their support domains. Suppose X and Y have N_x and N_y data points, and assume the sampling density ratio is $\frac{N_y}{N_x} = \alpha$. Before providing the proof of Theorem 1, we firstly prove Lemma 1, which will be used later.

Remark 4 The condition of most relevant equations in the proof is that the N_x and N_y are approaching infinity in the limit.

Lemma 1 *If and only if two classes X and Y have the same distribution covering region Ω and $\frac{N_y}{N_x} = \alpha$, for any sub-region $\Delta \subseteq \Omega$, with X and Y having n_{xi}, n_{yi} points, $\frac{n_{yi}}{n_{xi}} = \alpha$ holds.*

Proof Assume the distributions of X and Y are $f(x)$ and $g(y)$. In the union region of X and Y , arbitrarily take one tiny cell (region) Δ_i with $n_{xi} = \Delta_i f(x_i) N_x$, $n_{yi} = \Delta_i g(y_i) N_y$; $x_i = y_i$. Then,

$$\frac{n_{yi}}{n_{xi}} = \frac{\Delta_i g(x_i) N_y}{\Delta_i f(x_i) N_x} = \alpha \frac{g(x_i)}{f(x_i)}$$

Therefore:

$$\alpha \frac{g(x_i)}{f(x_i)} = \alpha \Leftrightarrow \frac{g(x_i)}{f(x_i)} = 1 \Leftrightarrow \forall x_i : g(x_i) = f(x_i)$$

□

2.4.1 Sufficient condition

Sufficient condition of Theorem 1. *If the two classes X and Y with the same distribution and have sufficient data points ($|X|$ and $|Y| \rightarrow \infty$), then the distributions of the ICD and BCD sets are nearly identical.*

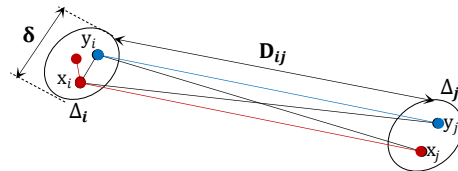


Fig. 4: Two non-overlapping small cells

Proof Within the area, select two tiny non-overlapping cells (regions) Δ_i and Δ_j (Figure 4). Since X and Y have the same distribution but in general different densities, the number of points in the two cells $n_{xi}, n_{yi}; n_{xj}, n_{yj}$ fulfills:

$$\frac{n_{yi}}{n_{xi}} = \frac{n_{yj}}{n_{xj}} = \alpha$$

The scale of cells is δ , the ICDs and BCDs of X and Y data points in cell Δ_i are approximately δ because the cell is sufficiently small. By the Definition 1 and 2:

$$d_{x_i} \approx d_{x_i, y_i} \approx \delta; \quad x_i, y_i \in \Delta_i$$

Similarly, the ICDs and BCDs of X and Y data points between cells Δ_i and Δ_j are approximately the distance between the two cells D_{ij} :

$$d_{x_{ij}} \approx d_{x_i, y_j} \approx d_{y_i, x_j} \approx D_{ij}; \quad x_i, y_i \in \Delta_i; \quad x_j, y_j \in \Delta_j$$

First, divide the whole distribution region into many non-overlapping cells. Arbitrarily select two cells Δ_i and Δ_j to examine the ICD set for X and the BCD set for X and Y . By Corollaries 1 and 2:

i) The ICD set for X has two distances: δ and D_{ij} , and their numbers are:

$$d_{x_i} \approx \delta; \quad x_i \in \Delta_i: \quad |\{d_{x_i}\}| = \frac{1}{2}n_{x_i}(n_{x_i} - 1)$$

$$d_{x_{ij}} \approx D_{ij}; \quad x_i \in \Delta_i; \quad x_j \in \Delta_j: \quad |\{d_{x_{ij}}\}| = n_{x_i}n_{x_j}$$

ii) The BCD set for X and Y also has two distances: δ and D_{ij} , and their numbers are:

$$d_{x_i, y_i} \approx \delta; \quad x_i, y_i \in \Delta_i: \quad |\{d_{x_i, y_i}\}| = n_{x_i}n_{y_i}$$

$$d_{x_i, y_j} \approx d_{y_i, x_j} \approx D_{ij}; \quad x_i, y_i \in \Delta_i; \quad x_j, y_j \in \Delta_j:$$

$$|\{d_{x_i, y_j}\}| = n_{x_i}n_{y_j}; \quad |\{d_{y_i, x_j}\}| = n_{y_i}n_{x_j}$$

Therefore, the proportions of the number of distances with a value of D_{ij} in the ICD and BCD sets are:

For ICDs:

$$\frac{|\{d_{x_{ij}}\}|}{|\{d_x\}|} = \frac{2n_{x_i}n_{x_j}}{N_x(N_x - 1)}$$

For BCDs, considering the density ratio:

$$\frac{|\{d_{x_i, y_j}\}| + |\{d_{y_i, x_j}\}|}{|\{d_{x, y}\}|} = \frac{\alpha n_{x_i}n_{x_j} + \alpha n_{x_i}n_{x_j}}{\alpha N_x^2} = \frac{2n_{x_i}n_{x_j}}{N_x^2}$$

The ratio of proportions of the number of distances with a value of D_{ij} in the two sets is:

$$\frac{N_x(N_x - 1)}{N_x^2} = 1 - \frac{1}{N_x} \rightarrow 1 \quad (N_x \rightarrow \infty)$$

This means that the number of proportions of the number of distances with a value of D_{ij} in the two sets is equal. We then examine the proportions of the number of distances with a value of δ in the ICD and BCD sets.

For ICDs:

$$\begin{aligned} \sum_i \frac{|\{d_{x_i}\}|}{|\{d_x\}|} &= \frac{\sum_i [n_{x_i}(n_{x_i} - 1)]}{N_x(N_x - 1)} \\ &= \frac{\sum_i (n_{x_i}^2 - n_{x_i})}{N_x^2 - N_x} = \frac{\sum_i (n_{x_i}^2) - N_x}{N_x^2 - N_x} \end{aligned}$$

For BCDs, considering the density ratio:

$$\sum_i \frac{|\{d_{x_i, y_i}\}|}{|\{d_{x, y}\}|} = \frac{\sum_i (n_{x_i}^2)}{N_x^2}$$

The ratio of proportions of the number of distances with a value of δ in the two sets is:

$$\begin{aligned} \frac{\sum_i (n_{x_i}^2)}{N_x^2} \cdot \frac{N_x^2 - N_x}{\sum_i (n_{x_i}^2) - N_x} \\ = \sum_i \left(\frac{n_{x_i}^2}{N_x^2} \right) \cdot \frac{1 - \frac{1}{N_x}}{\sum_i \left(\frac{n_{x_i}^2}{N_x^2} \right) - \frac{1}{N_x}} \rightarrow 1 \quad (N_x \rightarrow \infty) \end{aligned}$$

This means that the number of proportions of the number of distances with a value of δ in the two sets is equal.

In summary, the fact that the proportion of any distance value (δ or D_{ij}) in the ICD set for X and in the BCD set for X and Y is equal indicates that the distributions of the ICD and BCD sets are identical, and a corresponding proof applies to the ICD set for Y . \square

2.4.2 Necessary condition

Necessary condition of Theorem 1. *If the distributions of the ICD and BCD sets with sufficient data points ($|X|$ and $|Y| \rightarrow \infty$) are nearly identical, then the two classes X and Y must have the same distribution.*

Remark 5 We prove its **contrapositive**: if X and Y do not have the same distribution, the distributions of the ICD and BCD sets are not identical. We then apply proof by **contradiction**: suppose that X and Y do not have the same distribution, but the distributions of the ICD and BCD sets are identical.

Proof Suppose classes X and Y have the data points N_x, N_y , which $\frac{N_y}{N_x} = \alpha$. Divide their distribution area into many non-overlapping tiny cells (regions). In the i -th cell Δ_i , since distributions of X and Y are different, according to Lemma 1, the number of points in the cell n_{x_i}, n_{y_i} fulfills:

$$\frac{n_{y_i}}{n_{x_i}} = \alpha_i; \quad \exists \alpha_i \neq \alpha$$

The scale of cells is δ and the ICDs and BCDs of the X and Y points in cell Δ_i are approximately δ because the cell is sufficiently small.

$$d_{x_i} \approx d_{y_i} \approx d_{x_i, y_i} \approx \delta; \quad x_i, y_i \in \Delta_i$$

In the i -th cell Δ_i :

i) The ICD of X is δ , with a proportion of:

$$\begin{aligned} \sum_i \frac{|\{d_{x_i}\}|}{|\{d_x\}|} &= \frac{\sum_i [n_{x_i}(n_{x_i} - 1)]}{N_x(N_x - 1)} \\ &= \frac{\sum_i (n_{x_i}^2 - n_{x_i})}{N_x^2 - N_x} = \frac{\sum_i (n_{x_i}^2) - N_x}{N_x^2 - N_x} \quad (1) \end{aligned}$$

ii) The ICD of Y is δ , with a proportion of:

$$\begin{aligned} \sum_i \frac{|\{d_{y_i}\}|}{|\{d_y\}|} &= \frac{\sum_i [n_{y_i}(n_{y_i} - 1)]}{N_y(N_y - 1)} = \frac{\sum_i (n_{y_i}^2 - n_{y_i})}{N_y^2 - N_y} \\ &= \frac{\sum_i (n_{y_i}^2) - N_y}{N_y^2 - N_y} \Bigg|_{\substack{N_y = \alpha N_x \\ n_{y_i} = \alpha_i n_{x_i}}} = \frac{\sum_i (\alpha_i^2 n_{x_i}^2) - \alpha N_x}{\alpha^2 N_x^2 - \alpha N_x} \quad (2) \end{aligned}$$

iii) The BCD of X and Y is δ , with a proportion of:

$$\sum_i \frac{|\{d_{x_i, y_i}\}|}{|\{d_{x, y}\}|} = \frac{\sum_i (n_{x_i} n_{y_i})}{N_x N_y} = \frac{\sum_i (\alpha_i n_{x_i}^2)}{\alpha N_x^2} \quad (3)$$

For the distributions of the two sets to be identical, the ratio of proportions of the number of distances with a value of δ in the two sets must be 1, that is $\frac{(3)}{(1)} = \frac{(3)}{(2)} = 1$. Therefore:

$$\begin{aligned} \frac{(3)}{(1)} &= \frac{\sum_i (\alpha_i n_{x_i}^2)}{\alpha N_x^2} \cdot \frac{N_x^2 - N_x}{\sum_i (n_{x_i}^2) - N_x} \\ &= \frac{1}{\alpha N_x^2} \sum_i (\alpha_i n_{x_i}^2) \cdot \frac{1 - \frac{1}{N_x}}{\frac{1}{N_x^2} \sum_i (n_{x_i}^2) - \frac{1}{N_x}} \Bigg|_{N_x \rightarrow \infty} \\ &= \frac{1}{\alpha} \cdot \frac{\sum_i (\alpha_i n_{x_i}^2)}{\sum_i (n_{x_i}^2)} = 1 \quad (4) \end{aligned}$$

Similarly,

$$\begin{aligned} \frac{(3)}{(2)} &= \frac{\sum_i (\alpha_i n_{x_i}^2)}{\alpha N_x^2} \cdot \frac{\alpha^2 N_x^2 - \alpha N_x}{\sum_i (\alpha_i^2 n_{x_i}^2) - \alpha N_x} \\ &= \frac{\sum_i (\alpha_i n_{x_i}^2)}{N_x^2} \cdot \frac{\alpha - \frac{1}{N_x}}{\frac{1}{N_x^2} \sum_i (\alpha_i^2 n_{x_i}^2) - \frac{\alpha}{N_x}} \Bigg|_{N_x \rightarrow \infty} \\ &= \alpha \cdot \frac{\sum_i (\alpha_i n_{x_i}^2)}{\sum_i (\alpha_i^2 n_{x_i}^2)} = 1 \quad (5) \end{aligned}$$

To eliminate the $\sum_i (\alpha_i n_{x_i}^2)$ by considering the Eq. 4 and 5, we have:

$$\sum_i (n_{x_i}^2) = \frac{\sum_i (\alpha_i^2 n_{x_i}^2)}{\alpha^2}$$

Let $\rho_i = \left(\frac{\alpha_i}{\alpha}\right)^2$, then,

$$\sum_i (n_{x_i}^2) = \sum_i (\rho_i n_{x_i}^2)$$

Since n_{x_i} could be any value, to hold the equation requires $\rho_i = 1$. Hence:

$$\forall \rho_i = \left(\frac{\alpha_i}{\alpha}\right)^2 = 1 \Rightarrow \forall \alpha_i = \alpha$$

This contradicts $\exists \alpha_i \neq \alpha$. Therefore, the contrapositive proposition has been proved. \square

3 Experiments

We test our proposed DSI measure on two-class synthetic and multi-class real datasets and compare it with other complexity measures from the Extended Complexity Library (ECoL) package [17] in R. Since the DSI is computed using KS distances between the ICD and BCD sets, it ranges from 0 to 1. For separability, a higher DSI value means the dataset is easier to separate, *i.e.*, it has lower data complexity. Hence, to compare it with other complexity measures, we use $(1 - DSI)$. In this paper, higher complexity means lower separability (*i.e.* $Separability = 1 - Complexity$).

3.1 Two-class synthetic data

3.1.1 Typical datasets

In this section, we present the results of the DSI and the other complexity measures (listed in Table 1) for several typical two-class datasets. Figure 5 displays their plots and histograms of the ICD sets (for Class 1 and Class 2) and the BCD set (between Class 1 and Class 2). Each class consists of 1,000 data points.

Table 2 presents the results for these measures shown in Table 1 and our proposed DSI. The measures shaded in gray are considered to have failed in measuring separability and are not used for subsequent experiments. In particular, the *dimensionality* and *class-imbalance* measures do not work with separability in this situation. The *feature-based* and *linearity* measures measured the XOR dataset as having more complexity than the Random dataset; since the XOR has much clearer boundaries than Random between the two classes, these measures are inappropriate for measuring separability. N1 and N3 produce the same values for the Spiral, Moon, Circle, and Blob datasets, even though the Spiral dataset is obviously more difficult to separate than the Blob dataset, which is the most separable because a single line can be used to separate the two classes. However, the ClsCoef and Hubs measures assign the Blob dataset greater complexity than some other cases. In this experiment, N2, N4, T1, LSC, Density, and the proposed measure $(1 - DSI)$ are shown to accurately reflect the separability of these datasets.

3.1.2 Training distinctness (TD) and the two-cluster dataset

Definition 3 The training distinctness (TD) is the average training accuracy during the training process of a neural network classifier.

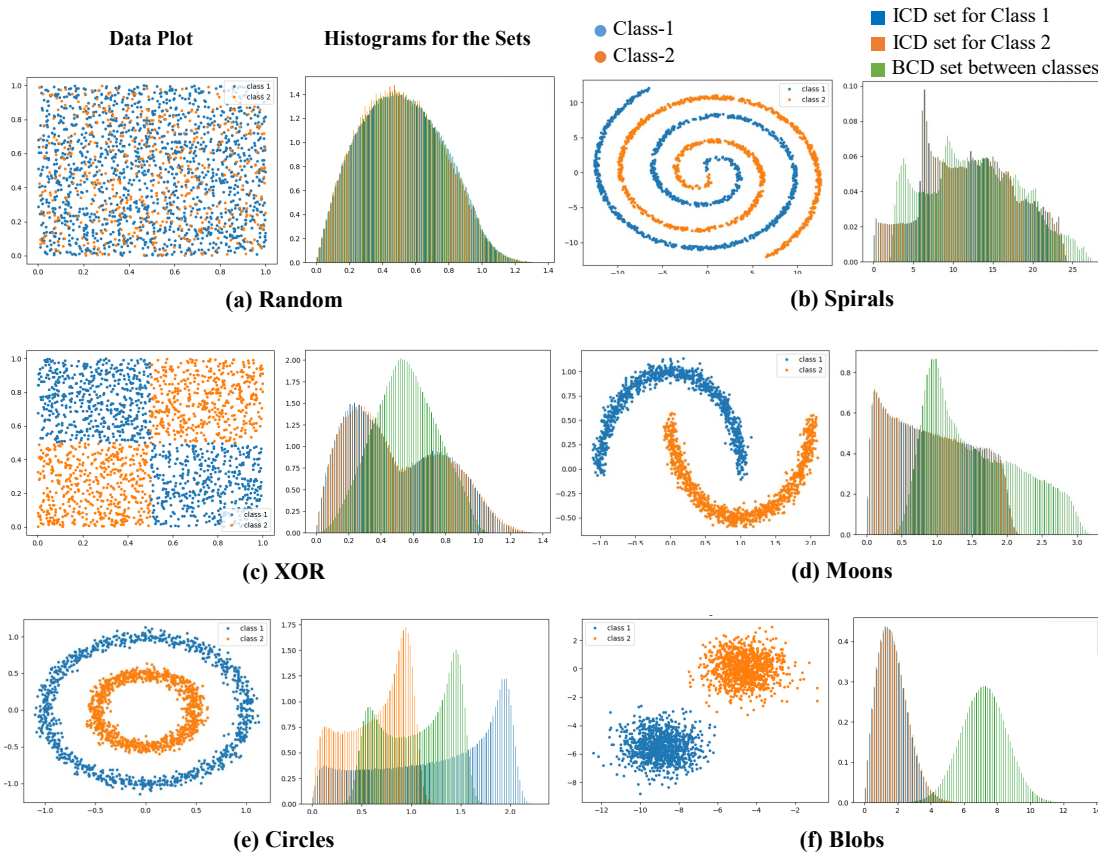


Fig. 5: Typical two-class datasets and their ICD and BCD set distributions

Remark 6 To quantify the difficulty of training the classifier, we define the training distinctness (TD). A lower TD value means that a dataset is more difficult to train, and this difficulty can reflect the separability of the dataset. Hence, TD is the baseline of data separability.

In this section, we synthesize a two-class dataset that has different separability levels. The dataset has two clusters, one for each class. The parameter controlling the standard deviation (SD) of clusters influences separability (Figure 6), and the baseline is the TD we defined.

We created nine two-class datasets using the `sklearn.datasets.make_blobs` function in Python. Each dataset has 2,000 data points (1,000 per class) and two cluster centers for the two classes, and the SD parameters of clusters are set from 1 to 9. Along with SD of clusters increasing, distributions of two classes are more overlapped and mixed together, thus reducing the separability of the datasets.

We use a simple fully-connected neural network (FCNN) model to classify these two-class datasets. This FCNN model has three hidden layers; there are 16,

32, and 16 neurons, respectively, with ReLU activation functions in each layer. The classifier was trained on one of the nine datasets, repeatedly from scratch. We set 1,000 epochs for each training session to compute the TD of each dataset.

In this case, separability could be clearly visualized by the complexity of the decision boundary. Figure 6 shows that datasets with a larger cluster SD need more complex decision boundaries. In fact, if a classifier model can produce decision boundaries for any complexity, it can achieve 100% training accuracy for any datasets (no two data points from different classes have all the same features) but the training steps (*i.e.* epochs) required to reach 100% training accuracy may vary. For a specific model, a more complex decision boundary may need more steps to train. Therefore, the average training accuracy throughout the training process – *i.e.* TD – can indicate the complexity of the decision boundary and the separability of the dataset.

Since the training accuracy ranges from 0.5 to 1.0 for two-class classification, to enable a comparison with other measures that range from 0 to 1, we normalize

Table 2: Complexity measures results for the two-class datasets (Figure 5). The measures shaded in grey failed to measure separability.

Category	Code	Random	Spirals	XOR	Moons	Circles	Blobs
Feature-based	F1	0.998	0.947	1.000	0.396	1.000	0.109
	F1v	0.991	0.779	0.999	0.110	1.000	0.019
	F2	0.996	0.719	0.996	0.151	0.329	0.006
	F3	0.997	0.843	0.998	0.397	0.708	0.007
	F4	0.995	0.827	0.997	0.199	0.500	0.000
Linearity	L1	0.201	0.170	0.328	0.074	0.233	0.000
	L2	0.485	0.407	0.487	0.114	0.458	0.000
	L3	0.469	0.399	0.486	0.055	0.454	0.000
Neighborhood	N1	0.719	0.001	0.040	0.001	0.001	0.001
	N2	0.502	0.052	0.071	0.025	0.043	0.017
	N3	0.500	0.000	0.019	0.000	0.000	0.000
	N4	0.450	0.359	0.152	0.099	0.162	0.000
	T1	0.727	0.045	0.043	0.008	0.012	0.001
	LSC	0.999	0.976	0.934	0.840	0.914	0.526
Network	Density	0.916	0.919	0.864	0.847	0.880	0.812
	ClsCoef	0.352	0.343	0.267	0.225	0.253	0.332
	Hubs	0.775	0.822	0.857	0.767	0.650	0.842
Dimensionality	T2	0.001	0.001	0.001	0.001	0.001	0.001
	T3	0.001	0.001	0.001	0.001	0.001	0.001
	T4	1.000	1.000	1.000	1.000	1.000	1.000
Class imbalance	C1	1.000	1.000	1.000	1.000	1.000	1.000
	C2	0.000	0.000	0.001	0.000	0.000	0.000
Proposed	$1 - DSI$	0.994	0.953	0.775	0.643	0.545	0.027

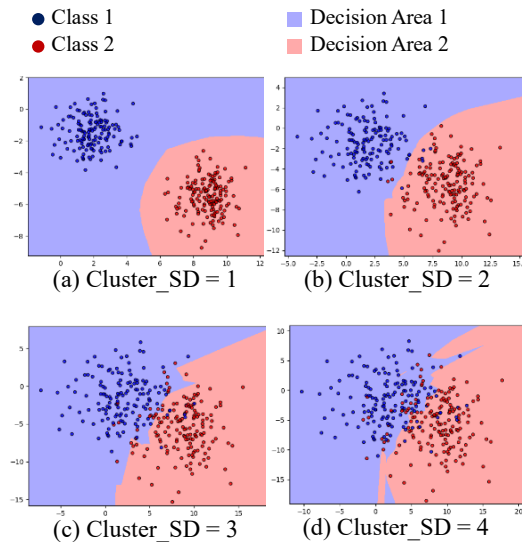


Fig. 6: Two-class datasets with different cluster standard deviation (SD) and trained decision boundaries.

the accuracy by the function:

$$r(x) = (x - 0.5)/0.5$$

$rTD = r(TD)$. The range of rTD is from 0 to 1, and the lowest complexity (highest separability) is 1. We also compute N2, N4, T1, LSC, Density, and the proposed measure $(1 - DSI)$ for the nine datasets and present them together with rTD as a baseline for separability in Figure 7.

As shown in Figure 7, the rTD for datasets with larger cluster SDs is lower. Lower rTD indicates lower separability and higher complexity. The measures N2, N4, T1, and the proposed measure $(1 - DSI)$ reflect the complexity of these datasets well, but the LSC and Density measures do not well reflect the complexity because they have relatively high values for the linearly separable dataset (Cluster_SD = 1, see Figure 6a) and increase very slightly for the Cluster_SD = 5 to Cluster_SD = 9 datasets. The measures N2, N4, and T1 perform similarly to each other. By comparison with them, $(1 - DSI)$ is the most sensitive measure to the change in separability and has the widest range.

3.2 CIFAR-10/100 datasets

We next use real images from the CIFAR-10/100 database [15] to examine the separability measures. A simple CNN with four convolutional layers, two max-

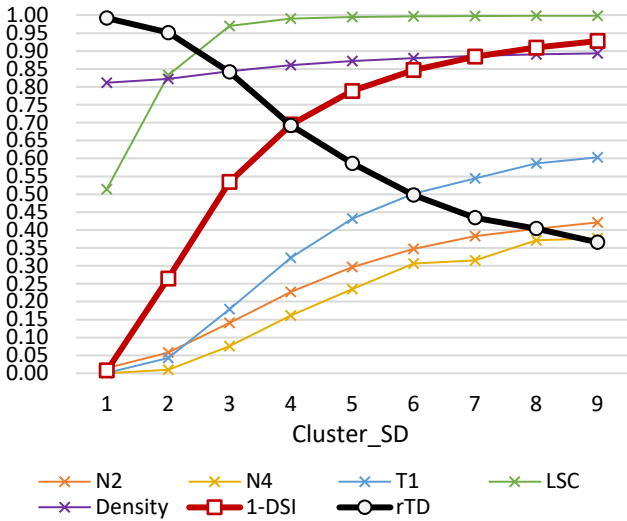


Fig. 7: Complexity measures for two-class datasets with different cluster SDs.

pooling layers, and one dense layer is trained to classify images; [Appendix: the CNN architecture for Cifar-10/100](#) presents its detailed architecture.

The CNN classifier is trained on 50,000 images from the CIFAR-10/100 database. To change the classification performance (*i.e.*, the TD), we apply several image pre-processing methods to the input images before training the CNN classifier. These pre-processing methods are supposed to change the distribution of the training images, and thus alter the separability of the dataset. And, the change of data separability will affect the classification results for the given CNN in terms of the TD.

3.2.1 Subsets and the DSI

Images in the CIFAR-10 dataset are grouped into 10 classes and the CIFAR-100 dataset consists of 20 super-classes. Both CIFAR-10 and CIFAR-100 consist of 50,000 images (32x32, 8-bit RGB), and each image has 3072 pixels (features).

Since to apply the measures using all 50,000 images would be very time-consuming (including the DSI, most of the measures have a time cost of $O(n^2)$), we randomly select subsets of 1/5, 1/10, 1/50, 1/100, and 1/500 of the original training images (*i.e.* without pre-processing) from CIFAR-10 and compute their DSIs. For each subset, we repeat the random selection and DSI computation eight times to calculate the mean and SD of DSIs. Figure 8 shows that the subset containing 1/50 training images or more does not significantly affect the measures. For example, the DSI for the whole (50,000) training images is 0.0945, while the

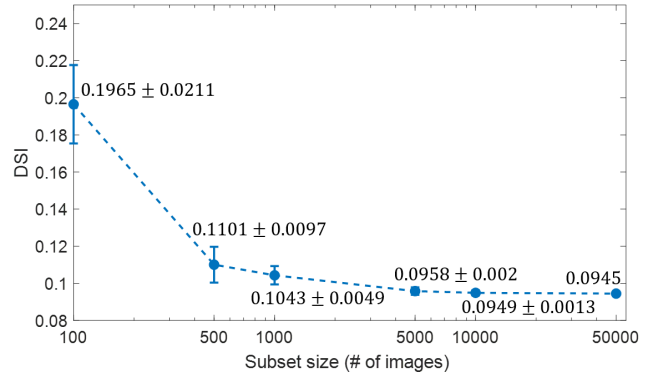


Fig. 8: DSIs of CIFAR-10 subsets

DSI for a subset of 1,000 randomly selected images is 0.1043 ± 0.0049 – the absolute difference is up to 0.015 (16%) but with an execution speed that is about 2,500 times greater: computing the DSI for 1,000 images requires about 30 seconds; for the whole training dataset, the DSI calculation requires about 20 hours. In addition, because the same subset is used for all measures, the comparison results are not affected. Therefore, we have randomly selected 1,000 training images to compute the measures, and this subset still accurately reflects the separability/complexity of the entire dataset.

3.2.2 Results

We use the functions in `PIL.ImageEnhance` (PIL is the Python Imaging Library) with five pre-processing methods applied to the original training images from CIFAR-10/100: Color (factor = 2) and Sharpness (2), Color (2), Contrast (2), Color (0.1), and Contrast (0.5). Including the original images, we use six image datasets to compute the DSI, TD, and other measures. For the 10-class classification, the training accuracy ranges from 0.1 to 1.0. The TD is not regularized in this section because it has a range close to $[0, 1]$.

Figure 9 shows the results for CIFAR-10 and CIFAR-100. The x-axis shows the pre-processing methods applied to the datasets, decreasingly ordered from left to right by TD, which is the baseline of data separability. Since a lower TD indicates lower separability and higher complexity, the values of complexity measures should strictly increase from left to right. We put specific values of measures in the Table 3 and 4 because some differences of complexity measures' results are small and not obviously shown by curves. By examining these values, we clearly find that the measures LSC, T1 (which almost overlaps with LSC) and Density have high values and remain nearly flat from left to right (insensitive), while N2 and N4 decrease

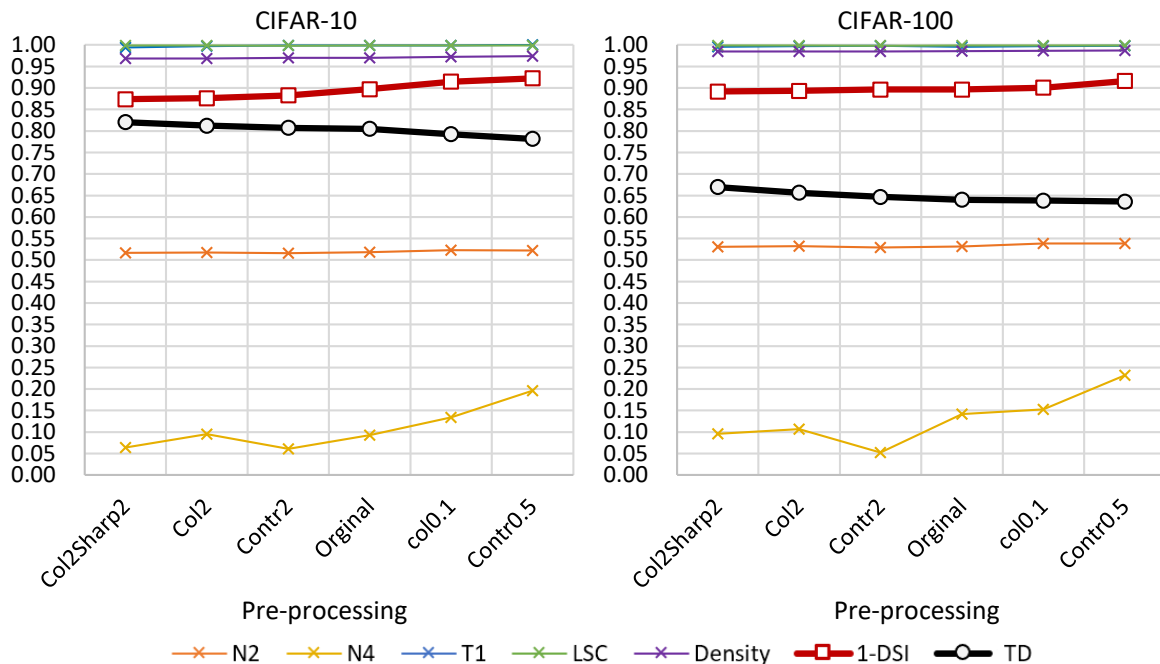


Fig. 9: Manipulation (*e.g.*, pre-processing) of images in datasets can change their complexities. We then simultaneously compare different methods of pre-processing and of complexity measures (the y-axes) including the *training distinctness* (TD) as ground truth, on the CIFAR-10/100 datasets. The x-axes show pre-processing methods, from left to right: Color (factor = 2) and Sharpness (2), Color (2), Contrast (2), Color (0.1), and Contrast (0.5).

for the Contrast (2) pre-processing stage. Unlike the other measures, $(1 - DSI)$ monotonically increases from left to right and correctly reflects (and is more sensitive to) the complexity of these datasets. These results show the advantage of DSI and indicate that image pre-processing is useful for improving CNN performance in image classification.

4 Discussion

4.1 Kolmogorov–Smirnov tests and other measures

It is noteworthy that our DSI is compatible with various measures of distances and distributions. The Euclidean distance and Kolmogorov–Smirnov (KS) distance are selected because, based on our experiments, we found that DSI has better sensitivity to separability by using those measures than by the other mentioned measures. The best sensitivity means the change of separability leads to the greatest difference of DSI.

One key step in DSI computation is to examine the similarity of the distributions of the ICD and BCD sets. We applied the KS distance in our study. The result of a two-sample KS distance is the maximum distance

between two cumulative distribution functions (CDFs):

$$KS(P, Q) = \sup_x |P(x) - Q(x)|$$

Where P and Q are the respective CDFs of the two distributions p and q .

Although many statistical measures, such as the Bhattacharyya distance, Kullback–Leibler divergence, and Jensen–Shannon divergence, could be used to compare the similarity between two distributions, most of them require the two sets to have the same number of data points. It is easy to show that the ICD and BCD sets ($|\{d_x\}|$, $|\{d_y\}|$, and $|\{d_{x,y}\}|$) cannot be the same size. For example, The f -divergence [21]:

$$D_f(P, Q) = \int q(x) f\left(\frac{p(x)}{q(x)}\right) dx$$

cannot be used to compute the DSI because the ICD and BCD have different numbers of values, thus the distributions p and q are in different domains. Measures based on CDFs can solve this problem because CDFs exist in the union domain of p and q . Therefore, the Wasserstein-distance [24] (W-distance) can be applied as an alternative similarity measure. For two 1-D distributions (*e.g.* ICD and BCD sets), the result of W-distance represents the difference in the area of the two

Table 3: Values of complexity measures for CIFAR-10

Method Code	Col2Sharp2	Col2	Contr2	Orginal	Col0.1	Contr0.5
N2	0.5169	0.5174	0.5158	0.5185	0.5226	0.5219
N4	0.0640	0.0950	0.0610	0.0930	0.1340	0.1960
T1	0.9940	0.9970	0.9990	0.9990	0.9990	1.0000
LSC	0.9985	0.9985	0.9984	0.9985	0.9986	0.9986
Density	0.9682	0.9684	0.9697	0.9701	0.9722	0.9737
1 - DSI	0.8739	0.8762	0.8829	0.8973	0.9147	0.9224
TD	0.8207	0.8122	0.8071	0.8051	0.7925	0.7818

Table 4: Values of complexity measures for CIFAR-100

Method Code	Col2Sharp2	Col2	Contr2	Orginal	Col0.1	Contr0.5
N2	0.5304	0.5324	0.5292	0.5315	0.5383	0.5386
N4	0.0960	0.1070	0.0520	0.1420	0.1530	0.2320
T1	0.9960	0.9970	0.9980	0.9960	0.9970	0.9980
LSC	0.9988	0.9988	0.9987	0.9988	0.9989	0.9988
Density	0.9849	0.9849	0.9851	0.9855	0.9867	0.9873
1 - DSI	0.8916	0.8933	0.8963	0.8964	0.9005	0.9160
TD	0.6696	0.6563	0.6466	0.6403	0.6380	0.6359

CDFs:

$$W_1(P, Q) = \int |P(x) - Q(x)| dx$$

The DSI uses the KS distance rather than the W-distance because we find that normalized W-distance is not as sensitive as the KS distance for measuring separability. To illustrate this, we compute the DSI by using the two distribution measures for the nine two-cluster datasets in Section 3.1.2. The two DSIs are then compared by the baseline rTD, which is also used in Section 3.1.2. Figure 10 shows that along with the separability of the datasets decreasing, KS distance has a wider range of decrease than the W-distance. Hence, the KS distance is considered a better distribution measure for the DSI in terms of revealing differences in the separability of datasets.

4.1.1 Distance metrics

Since the DSI examines the distributions of distances between data points, the used distance metric is another important factor. In this study, the DSI uses the Euclidean distance because it has better sensitivity to separability. We also tested several other commonly used distance metrics: City-block, Chebyshev, Correlation, Cosine, and Mahalanobis distances. We computed the DSIs based on these distance metrics using the nine two-cluster datasets in Section 3.1.2 and the results are compared by the baseline rTD. Figure 11 shows that the Euclidean distance performs similarly as the City-block and Chebyshev distances. Such results indicate

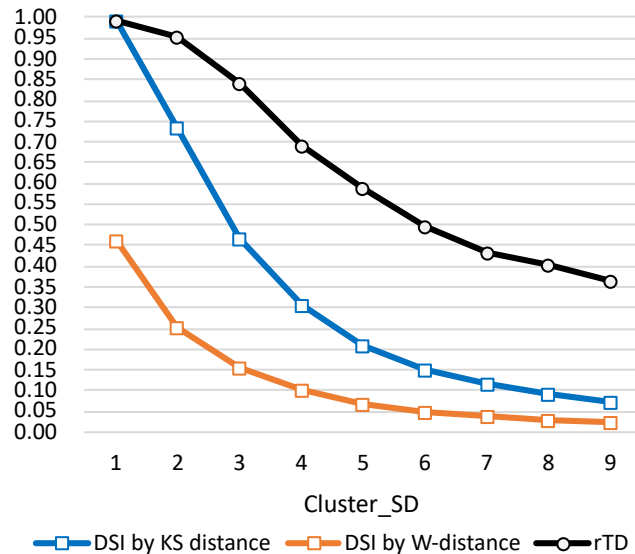


Fig. 10: DSI calculation using different distribution measures.

that the Minkowski distance metric (p -norm) could be suitable for the computation of DSI.

4.2 Significance and contributions

This work is motivated by the need for a new metric to measure the difficulty of a dataset to be classified by machine learning models. This measure of a dataset's separability is an intrinsic characteristic of a dataset, in-

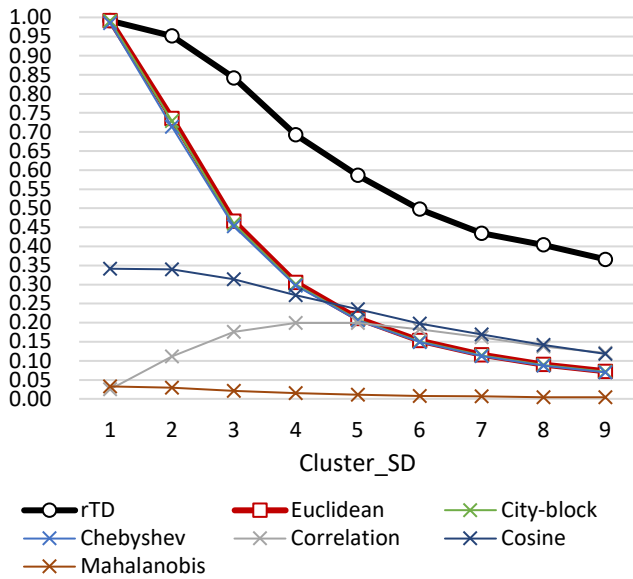


Fig. 11: DSI calculation using different distance metrics.

dependent of classifier models, that describes how data points belonging to different classes are mixed. To measure the separability of mixed data points of two classes is essentially to evaluate whether the two datasets are from the same distribution. According to Theorem 1, the DSI provides **an effective way to verify whether the distributions of two sample sets are identical for any dimensionality**.

As discussed in Section 2, if the DSI of sample sets is close to zero, the very low separability means that the two classes of data are scattered and mixed together with nearly the same distribution. The DSI transforms the comparison of distributions problem in R^n (for two sample sets) to the comparison of distributions problem in R^1 (*i.e.*, ICD and BCD sets) by computing the distances between samples. For example, in Figure 5(a), samples from Class 1 and 2 come from the same uniform distribution in R^2 over $[0, 1]^2$. Consequently, the distributions of their ICD and BCD sets are almost identical and the DSI is about 0.0058. In this case, each class has 1,000 data points. For twice the number of data points, the DSI decreases to about 0.0030. When there are more data points of two classes from the same distribution, the DSI will approach zero, which is the limit of the DSI if the distributions of two sample sets are identical.

4.3 Other applications and future works

The principal use of the proposed DSI is understanding data separability, which could help in choosing a proper

machine learning model for data classification [8]. This will be useful to the model designer who can begin with either a small- or large-scale classifier. For example, a simpler classifier could be used for an easily-separable dataset and thus reduce both computational cost and overfitting. DSI could serve also as a way to benchmark the efficiency of a classifier, given a suitable measure of classifier complexity and computational cost.

Since DSI can evaluate whether two datasets are from the same distribution, we have applied it [12] to evaluate generative adversarial networks (GANs) [9], competing with the existing IS and FID [13] measures. As with the FID, measuring how close the distributions of real and GAN-generated images are to each other is an effective approach to assess GAN performance because the goal of GAN training is to generate new images that have the same distribution as real images. We have also applied the DSI [11] as an internal cluster validity index (CVI) [2] to evaluate clustering results because the goal of clustering is to separate a dataset into clusters, in the macro-perspective, how well a dataset has been separated could be indicated via the separability of clusters.

By examining the similarity of the two distributions, the DSI can detect (or certify) the distribution of a sample set, *i.e.*, distribution estimation. Several distributions could be assumed (*e.g.*, uniform or Gaussian) and a test set is created with an assumed distribution. The DSI could then be calculated using the test and sample sets. The correct assumed distribution will have a very small DSI (*i.e.*, close to 0) value.

In addition to the mentioned applications, DSI can also be used as a feature-selection method for dimensionality reduction and an anomaly detection method in data analysis. DSI has broad applications in deep learning, machine learning, and data science beyond direct quantification of separability.

4.4 Limitations

Although DSI works for any dimensionality, dimensionality can affect data distributions and the measurement of distance, which is known as the curse of dimensionality [25], thus affecting the DSI. More studies should address the impact of dimensions on DSI and how to compare separability across different numbers of dimensions.

The separability in DSI is defined by the global distributions of data. In some cases, such separability cannot accurately reflect the complexity of the decision boundary because of local conditions. For example, in Figure 12, two datasets have approximately the

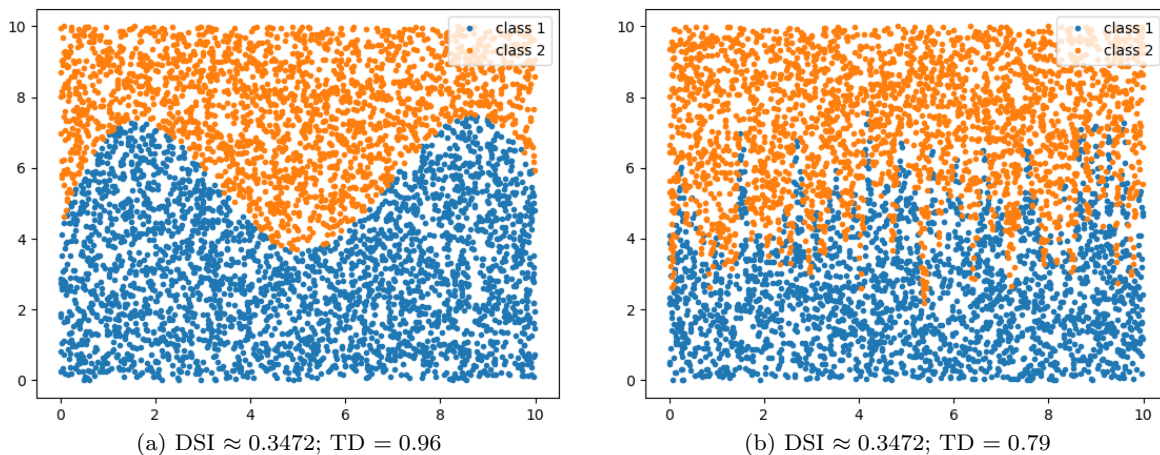


Fig. 12: Two-class datasets with different decision boundaries. They have the same DSI but different training distinctness (TD). The dataset (b) having more complex decision boundary is more difficult to be classified.

same DSI but the decision boundary complexity of the right dataset (b) is higher and its TD (by reusing the previous three-layer FCNN model in Section 3.1.2) is smaller. Therefore, the distribution-based separability cannot represent the general training/classification difficulty in terms of the complexity of decision boundaries. One of our studies addresses this problem by examining the complexity of data points on or near the decision boundary [10].

5 Conclusion

We proposed a novel and effective measure (**DSI**) to verify whether the distributions of two sample sets are identical for any dimensionality. This measure has a solid theoretical basis. The core **Theorem** we proved connects the distributions of two-class datasets with the distributions of their intra-class distance (**ICD**) sets and between-class distance (**BCD**) set. Usually, the datasets are in high-dimensional space and thus to compare their distributions is very difficult. By our theorem, to show that the distributions of two-class datasets are identical is equivalent to showing that the distributions of their ICD and BCD sets are identical. The distributions of sets are easy to compare because the distances are in R^1 . The DSI is based on the KS distance between these distances' sets.

DSI has many applications. This paper shows its core application, which is an intrinsic separability/complexity measure of a dataset. We consider that different classes of data that are mixed with the same distribution constitute the most difficult case to separate using classifiers. The DSI can indicate whether data belonging to different classes have the same dis-

tribution, and thus provides a measure of the separability of datasets. Quantification of the data separability could help a user choose a proper machine learning model for data classification without excessive iteration. Comparisons using synthetic and real datasets show that DSI performs better than many state-of-the-art separability/complexity measures and demonstrate its competitiveness as a useful measure.

Other important applications could be distribution estimation, feature selection, anomaly detection, evaluation of GANs, and playing the role of an internal cluster validity index to evaluate clustering results.

Appendix: the CNN architecture for Cifar-10/100

The CNN architecture used in Section 3.2 of the main paper consists of four convolutional layers, two max-pooling layers, and two fully connected (FC) layers. The activation function for each convolutional layer is the ReLU function, and that for output is softmax function, which maps the output value to a range of $[0, 1]$, with a summation of 1. The notation **Conv_3-32** indicates that there are 32 convolutional neurons (units), and the filter size in each unit is 3×3 pixels (height \times width) in this layer. **MaxPooling_2** denotes a max-pooling layer with a filter of 2×2 pixels window and stride 2. In addition, **FC_n** represents a FC layer with n units. The dropout layer randomly sets the fraction rate of the input units to 0 for the next layer with every update during training; this layer helps the network to avoid overfitting. Table 5 shows the detailed architecture. Our training optimizer is RMSprop [29] with a learning rate of $1e-4$ and a decay of $1e-6$, the loss function is categor-

Table 5: The CNN architecture used in Section 3.2

Layer	Shape
Input: RGB image	$32 \times 32 \times 3$
Conv_3-32 + ReLU	$32 \times 32 \times 32$
Conv_3-32 + ReLU	$32 \times 32 \times 32$
MaxPooling_2 + Dropout (0.25)	$16 \times 16 \times 32$
Conv_3-64 + ReLU	$16 \times 16 \times 64$
Conv_3-64 + ReLU	$16 \times 16 \times 64$
MaxPooling_2 + Dropout (0.25)	$8 \times 8 \times 64$
Flatten	4096
FC_512 + Dropout (0.5)	512
FC_10 (Cifar-10) / FC_20 (Cifar-100)	10 / 20
Output (softmax): [0,1]	10 (Cifar-10) / 20 (Cifar-100)

ical cross-entropy, the updating metric is accuracy, the batch size is 32, and the number of total epochs is set at 200.

Compliance with ethical standards

Conflict of interest The authors declare that they have no conflict of interest.

References

1. A., Z.D., Stéphane, L., Fabrice, M.: Separability index in supervised learning. Lecture Notes in Computer Science, pp. 475–487. Springer Berlin Heidelberg (2002)
2. Arbelaitz, O., Gurrutxaga, I., Muguerza, J., Pérez, J.M., Perona, I.: An extensive comparative study of cluster validity indices. *Pattern Recognition* **46**(1), 243–256 (2013). DOI <https://doi.org/10.1016/j.patcog.2012.07.021>. URL <https://www.sciencedirect.com/science/article/pii/S003132031200338X>
3. Brun, A.L., Britto, A.S., Oliveira, L.S., Enembreck, F., Sabourin, R.: Contribution of data complexity features on dynamic classifier selection. pp. 4396–4403. 2016 International Joint Conference on Neural Networks (IJCNN), IEEE, Vancouver, BC, Canada (2016). DOI 10.1109/IJCNN.2016.7727774. URL <http://ieeexplore.ieee.org/document/7727774/>
4. Brun, A.L., Britto, A.S., Oliveira, L.S., Enembreck, F., Sabourin, R.: A framework for dynamic classifier selection oriented by the classification problem difficulty. *Pattern Recognition* **76**, 175–190 (2018). DOI 10.1016/j.patcog.2017.10.038
5. Daboor, Howell, S., Shokr, Yackel, J.: The jefries-matusita distance for the case of complex wishart distribution as a separability criterion for fully polarimetric sar data. *International Journal of Remote Sensing* **35** (2014). DOI 10.1080/01431161.2014.960614
6. Fernández, A., García, S., Galar, M., Prati, R.C., Krawczyk, B., Herrera, F.: Data Intrinsic Characteristics. In: Learning from Imbalanced Data Sets, pp. 253–277. Springer International Publishing, Cham (2018). DOI 10.1007/978-3-319-98074-4_10. URL http://link.springer.com/10.1007/978-3-319-98074-4_10
7. Frank J. Massey, J.: The Kolmogorov-Smirnov Test for Goodness of Fit. *Journal of the American Statistical Association* **46**(253), 68–78 (1951). DOI 10.1080/01621459.1951.10500769
8. Garcia, L.P.F., Lorena, A.C., de Souto, M.C.P., Ho, T.K.: Classifier recommendation using data complexity measures. pp. 874–879. 2018 24th International Conference on Pattern Recognition (ICPR), IEEE, Beijing (2018). DOI 10.1109/ICPR.2018.8545110. URL <https://ieeexplore.ieee.org/document/8545110/>
9. Goodfellow, I., Pouget-Abadie, J., Mirza, M., Xu, B., Warde-Farley, D., Ozair, S., Courville, A., Bengio, Y.: Generative adversarial nets. In: Z. Ghahramani, M. Welling, C. Cortes, N.D. Lawrence, K.Q. Weinberger (eds.) *Advances in Neural Information Processing Systems* 27, p. 2672–2680. Curran Associates, Inc. (2014). URL <http://papers.nips.cc/paper/5423-generative-adversarial-nets.pdf>
10. Guan, S., Loew, M.: Analysis of generalizability of deep neural networks based on the complexity of decision boundary. In: 2020 19th IEEE International Conference on Machine Learning and Applications (ICMLA), pp. 101–106 (2020). DOI 10.1109/ICMLA51294.2020.00025
11. Guan, S., Loew, M.: An internal cluster validity index using a distance-based separability measure. In: 2020 IEEE 32nd International Conference on Tools with Artificial Intelligence (ICTAI), pp. 827–834 (2020). DOI 10.1109/ICTAI50040.2020.00131
12. Guan, S., Loew, M.: A novel measure to evaluate generative adversarial networks based on direct analysis of generated images. *Neural Computing and Applications* pp. 1–16 (2021)
13. Heusel, M., Ramsauer, H., Unterthiner, T., Nessler, B., Hochreiter, S.: Gans trained by a two time-scale update rule converge to a local nash equilibrium. In: I. Guyon, U.V. Luxburg, S. Bengio, H. Wallach, R. Fergus, S. Vishwanathan, R. Garnett (eds.) *Advances in Neural Information Processing Systems* 30, p. 6626–6637. Curran Associates, Inc. (2017)
14. Ho, T.K., Basu, M.: Complexity measures of supervised classification problems. *IEEE Transactions on Pattern Analysis and Machine Intelligence* **24**(3), 289–300 (2002). DOI 10.1109/34.990132
15. Krizhevsky, A.: Learning multiple layers of features from tiny images. Tech. rep. (2009)
16. Li, C., Wang, B.: Fisher linear discriminant analysis (2014)
17. Lorena, A.C., Garcia, L.P.F., Lehmann, J., Souto, M.C.P., Ho, T.K.: How complex is your classification

- problem?: A survey on measuring classification complexity. *ACM Comput. Surv.* **52**(5), 107:1–107:34 (2019). DOI 10.1145/3347711
18. Mishra, A.K.: Separability indices and their use in radar signal based target recognition. *IEICE Electronics Express* **6**(14), 1000–1005 (2009). DOI 10.1587/elex.6.1000
 19. Mthembu, L., Marwala, T.: A note on the separability index (2009)
 20. Nishikawa, S., Nojima, Y., Ishibuchi, H.: Appropriate granularity specification for fuzzy classifier design by data complexity measures. pp. 691–696. 2010 Second World Congress on Nature and Biologically Inspired Computing (NaBIC 2010), IEEE, Fukuoka (2010). DOI 10.1109/NABIC.2010.5716371. URL <http://ieeexplore.ieee.org/document/5716371/>
 21. Nowozin, S., Cseke, B., Tomioka, R.: f-gan: Training generative neural samplers using variational divergence minimization. In: *Proceedings of the 30th International Conference on Neural Information Processing Systems*, pp. 271–279 (2016)
 22. Pang, G., Shen, C., Cao, L., Hengel, A.V.D.: Deep learning for anomaly detection: A review. *ACM Comput. Surv.* **54**(2) (2021). DOI 10.1145/3439950. URL <https://doi.org/10.1145/3439950>
 23. Peterson, A.D.: A separability index for clustering and classification problems with applications to cluster merging and systematic evaluation of clustering algorithms. Ph.D. thesis, Ames, IA, USA (2011)
 24. Ramdas, A., Trillos, N.G., Cuturi, M.: On wasserstein two-sample testing and related families of nonparametric tests. *Entropy* **19**(2), 47 (2017)
 25. Rust, J.: Using randomization to break the curse of dimensionality. *Econometrica: Journal of the Econometric Society* pp. 487–516 (1997)
 26. Shannon, C.E.: A mathematical theory of communication. *The Bell System Technical Journal* **27**(3), 379–423 (1948). DOI 10.1002/j.1538-7305.1948.tb01338.x
 27. Sotoca, J., Sánchez, J., Mollineda, R.: A review of data complexity measures and their applicability to pattern classification problems. *Actas del III Taller Nacional de Minería de Datos y Aprendizaje* (2005)
 28. Thornton, C.: Separability is a learner’s best friend. In: J.A. Bullinaria, D.W. Glasspool, G. Houghton (eds.) *4th Neural Computation and Psychology Workshop*, London, 9–11 April 1997, pp. 40–46. Springer London, London (1998). URL http://link.springer.com/10.1007/978-1-4471-1546-5_4
 29. Tieleman, T., Hinton, G.: Lecture 6.5-rmsprop: Divide the gradient by a running average of its recent magnitude. *COURSERA: Neural networks for machine learning* **4**(2), 26–31 (2012)
 30. Zhang, C., Bengio, S., Hardt, M., Recht, B., Vinyals, O.: Understanding deep learning (still) requires rethinking generalization. *Commun. ACM* **64**(3), 107–115 (2021). DOI 10.1145/3446776. URL <https://doi.org/10.1145/3446776>